Reactivity of α-Phosphino Enolate Complexes of Nickel(II) and Palladium(II) toward Electrophilic Metal Centers. Synthesis and Crystal Structures of the Bimetallic Palladium(II)−Gold(I) Complex [(dmba)Pd{$Ph_2PCH(AuPPh_3)C(O)Ph$}](BF_4) and of the Nickel(II)−Cobalt(II) Paramagnetic Complex *cis*-[Ni{Ph_2PCH···$C(···O)(p\text{-}C_6H_4CH_3$}$_2$]$CoI_2$

Jacques Andrieu,[†] Pierre Braunstein,*[,†] Marc Drillon,[‡] Yves Dusausoy,[§] Florent Ingold,[†] Pierre Rabu,[‡] Antonio Tiripicchio,[||] and Franco Ugozzoli[||]

Laboratoire de Chimie de Coordination, Associé au CNRS (URA 416), Université Louis Pasteur, 4 rue Blaise Pascal, F-67070 Strasbourg Cédex, France, Groupe des Matériaux Inorganiques, IPCMS, rue du Loess, 67037 Strasbourg Cedex, Laboratoire de Cristallographie et Modélisation des Matériaux Minéraux et Biologiques, Associé au CNRS (URA 809), Université Henri Poincaré Nancy 1, B.P. 239, F-54506 Vandoeuvre-les-Nancy Cédex, France, and Dipartimento di Chimica Generale ed Inorganica, Chimica Analitica, Chimica Fisica, Centro di Studio per la Strutturistica Diffrattometrica del CNR, Università di Parma, Viale delle Scienze, I-43100 Parma, Italy

Received October 18, 1995[⊗]

The chemoselective reactivity of metal-coordinated phosphino enolates has been studied by the reactions of *cis*-[Ni{R'_2PCH···$C(···O)R$}$_2$] (R = Ph, *p*-C_6H_4Me, Me; R′ = Ph, ^{i}Pr, not all combinations) and [(C N)-Pd{Ph_2PCH···$C(···O)Ph$}] (C N = *o*-$C_6H_4CH_2NMe_2$, dmba or $C_{10}H_8N$, 8-mq) with different metal electrophiles. In the reaction of *cis*-[Ni{Ph_2PCH···$C(···O)Ph$}$_2$] (**1a**) with [$PtCl_2$(COD)] (COD = 1,5-cyclooctadiene), a transmetalation of the *P*,*O* ligands was observed, yielding the known complex *cis*-[Pt{Ph_2PCH···C-(···O)Ph}$_2$] (**3**). However, reaction of *cis*-[Ni{R'_2PCH···$C(···O)R$}$_2$] with anhydrous CoI_2 afforded the heterobinuclear complexes *cis*-[Ni{R'_2PCH···$C(···O)R$}$_2$]CoI_2 (**5a**, R = Ph, R′ = Ph; **5b,** R = *p*-C_6H_4Me, R′ = Ph; **5c**, R = Me, R′ = Ph; **7**, R = Ph, R′ = ^{i}Pr) which contain the phosphino enolate ligand in an unusual chelating-bridging μ-$\eta^1(O)$:$\eta^2(P,O)$ coordination mode in a nonplanar NiO_2Co unit. The magnetic properties of these complexes are discussed. The SHOP-type catalyst [Ni(Ph){Ph_2PCH···$C(···O)Ph$}(PPh_3)] also behaved as an oxygen-donor metalloligand toward CoI_2 to give a paramagnetic Co(II) complex. In contrast, reaction of [(C N)Pd{Ph_2PCH···$C(···O)Ph$}] with [$Au(PPh_3)$]$^+$ occurred with formation of [(dmba)-Pd{$Ph_2PCH(AuPPh_3)C(O)Ph$}](BF_4) (**4a**) in which a $C_{enolate}$−Au bond has been formed while the *P*,*O* chelate has remained coordinated to palladium. This reaction generates a new stereogenic center, as also evidenced by ^{1}H NMR spectroscopy. The solid state structures of complexes **4a**·$^1/_2C_7H_8$ and **5b**·CH_2Cl_2 have been determined by single-crystal X-ray diffraction: **4a**·$^1/_2C_7H_8$ crystallizes in the triclinic space group $P\bar{1}$ with $Z = 2$ in a unit cell of dimensions $a = 16.778(4)$ Å, $b = 14.269(5)$ Å, $c = 10.838(6)$ Å, $\alpha = 79.27(4)°$, $\beta = 71.59(3)°$, and $\gamma = 72.68(2)°$; **5**·CH_2Cl_2 crystallizes in the monoclinic space group $P2_1/n$ with $Z = 4$ in a unit cell of dimensions $a = 12.940(1)$ Å, $b = 18.329(2)$ Å, $c = 18.495(2)$ Å, and $\beta = 91.627(8)°$. The structures have been solved from diffractometer data by direct and Fourier methods and refined by full-matrix least-squares methods on the basis of 7240 (**4a**·$^1/_2C_7H_8$) and 3644 (**5b**·CH_2Cl_2) observed reflections to R and R_w values of 0.0363 and 0.0406 (**4a**·$^1/_2C_7H_8$) and 0.040 and 0.038 (**5b**·CH_2Cl_2), respectively.

Introduction

Although the chelating α-phosphino enolate-type ligand present in Ni-based homogeneous catalysts used in the SHOP process is assigned a spectator role during catalysis,[1] we have shown previously that the reactivity of α-phosphino enolates of the type [Ph_2PCH···$C(···O)R$]$^-$ (R = Ph, OEt, NPh_2)$^{2-5}$

[†] Université Louis Pasteur.
[‡] IPCMS.
[§] Université Henri Poincaré Nancy 1.
[||] Università di Parma.
[⊗] Abstract published in *Advance ACS Abstracts,* September 1, 1996.

(1) (a) Keim, W. *New J. Chem.* **1987**, *11*, 531. (b) Klabunde, U.; Tulip, T. H.; Roe, D. C.; Ittel, S. D. *J. Organomet. Chem.* **1987**, *334*, 141−156. (c) Hirose, K.; Keim, W. *J. Mol. Catal.* **1992**, *73*, 271−276.
(2) (a) Braunstein, P.; Matt, D.; Dusausoy, Y.; Fischer, J.; Mitschler, A. and Ricard, L. *J. Am. Chem. Soc.* **1981**, *103*, 5115−5125. (b) Braunstein, P.; Matt, D.; Nobel, D. *Chem. Rev.* **1988**, *88*, 747−764.

S0020-1669(95)01349-8 CCC: $12.00

Scheme 1

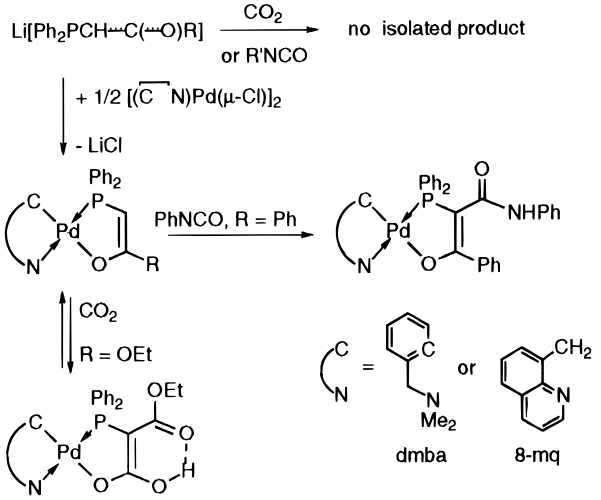

depends very much on the associated countercation. Whereas palladium(II) complexes have been shown to readily react with e.g. CO_2,[2] organic isocyanates,[3] or activated alkynes such as $MeO_2C{-}C{\equiv}C{-}CO_2Me$[4] by formation of a carbon-carbon bond, the alkali metal salts for example are surprisingly unreactive toward these heterocumulenes (Scheme 1). These observations have been rationalized on the basis of favorable electronic interactions involving the d^8 metal center.[6] Square-planar bis(phosphino enolate) complexes of Ni, Pd, and Pt have also been prepared and shown to react with organic isocyanates or $MeO_2C{-}C{\equiv}C{-}CO_2Me$ (reactivity order M = Ni > Pd > Pt) in a Michael-type addition resulting from nucleophilic attack of the enolate carbon on the appropriate carbon of the organic electrophile.[4] In contrast, with reagents such as Ph_2PCl or $PhPCl_2$, formation of a P−O bond occurs, leading e.g. to complexes containing the phosphine, phosphinite ligand $Ph_2PCH{=}C(Ph)OPPh_2$.[7 b−d] In order to further evaluate the chemoselectivity of reactions involving these coordinated phosphino enolate ligands, we decided to investigate reactions which could also provide an interesting access to new heterometallic complexes. Thus, reaction of [(C N)Pd{$Ph_2PCH{\cdots}C(\cdots O)OEt$}] (C N= dimethylbenzylamine (dmba) or 8-methylquinoleine (8-mq)) with [(C N)Pd(μ-Cl)]$_2$ in a 2:1 molar ratio afforded a dinuclear complex in which the phosphino enolate ligand has changed its coordination mode from η^2-*P,O* to μ-*P,C* (eq 1):[2a] However, reaction of *cis*-[Ni{$Ph_2PCH{\cdots}C(\cdots O)Ph$}$_2$] with [(C N)Pd($\mu$-Cl)]$_2$ yielded

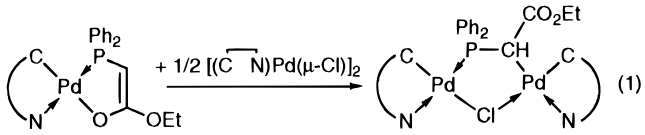

[(C N)Pd{$Ph_2PCH{\cdots}C(\cdots O)Ph$}] (C N= 8-mq) instead of a heterodinuclear complex (eq 2).[7c] Here we describe further

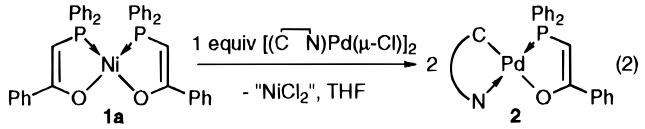

studies and report the crystal structures of Pd−Au and Ni−Co complexes which illustrate a different chemoselectivity of the enolate moiety. Note that *cis*-[Ni{$Ph_2PCH{\cdots}C(\cdots O)Ph$}$_2$] has been converted previously to an active ethylene homopolymerization catalyst by alkylation with trimethylaluminum.[8]

Results

A transmetalation reaction of the anionic *P,O* chelate of the type shown in eq 2 has now also been observed in the case of Pt since reaction of **1a** with [$PtCl_2$(COD)] afforded the known complex *cis*-[Pt{$Ph_2PCH{\cdots}C(\cdots O)Ph$}$_2$] (**3**)[7c] (details in the Experimental Section) (eq 3). Transfer of the chelating ligand

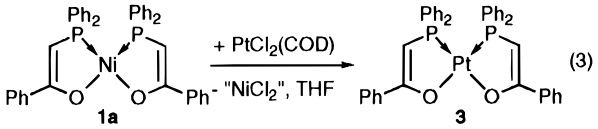

from Ni to Pd or Pt obviously occurs under thermodynamic control.

Synthesis and Structure of Pd(II)−Au(I) Complexes. Reaction of the neutral complexes [(C N)Pd{$Ph_2PCH{\cdots}C(\cdots O)Ph$}] with [Au($PPh_3$)]$^+$ yielded complexes **4** in which the gold atom is bonded to the former sp^2 carbon of the enolate which has become sp^3 hybridized and chiral in **4** (eq 4).

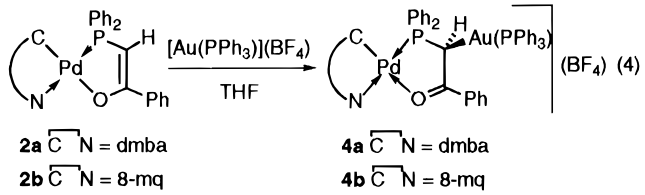

Accordingly, the ^{1}H NMR spectrum of **4a** contains a triplet resonance at δ 5.23 for the PCH proton ($^2J(P_{Pd}H) \sim {}^3J(P_{Au}H)$ = 8.2 Hz) and an ABX spin system for the NCH_2 protons. Since the keto functionality has been restored in this reaction, one would anticipate to find in the IR spectrum a ν(C=O) absorption around 1570 cm^{-1}, as in the analoguous complex [(C N)Pd{$Ph_2PCH_2C(O)Ph$}]$^+$ [7a] (remember the isolobal analogy between Au(PPh_3) and H). Instead, this absorption was found at 1510 cm^{-1}. The larger mass and/or the electronic effect of the AuL substituent could be responsible for this shift. Similar properties have been found for **4b** whose synthesis has been reported

(3) (a) Bouaoud, S.-E.; Braunstein, P.; Grandjean, D.; Matt, D.; Nobel, D. *J. Chem. Soc., Chem. Commun.* **1987**, 488−490. (b) Bouaoud, S.-E.; Braunstein, P.; Grandjean, D.; Matt, D.; Nobel, D. *Inorg. Chem.* **1988**, *27*, 2279−2286. (c) Braunstein, P.; Nobel, D. *Chem. Rev.* **1989**, *89*, 1927−1945.

(4) (a) Balegroune, F. Braunstein, P.; Gomes Carneiro, T. M.; Grandjean, D.; Matt, D. *J. Chem. Soc., Chem. Commun.* **1989**, 582−583. (b) Braunstein, P.; Gomes Carneiro, T. M.; Balegroune, F.; Grandjean, D. *Organometallics* **1989**, *8*, 1737−1743.

(5) (a) Andrieu, J.; Braunstein, P.; Tiripicchio, A.; Ugozzoli, F. *Inorg. Chem.* **1996**, *35*, 0000−0000. (b) Andrieu, J.; Braunstein, P.; Dusausoy, Y.; Ghermani, N. E. *Inorg. Chem.*, in press.

(6) Veya, P.; Floriani, C.; Chiesi-Villa, A.; Guastini, C.; Dedieu, A.; Ingold, F. and Braunstein, P. *Organometallics* **1993**, *12*, 4359−4367.

(7) (a) Bouaoud, S.-E.; Braunstein, P.; Grandjean, D.; Matt, D.; Nobel, D. *Inorg. Chem.* **1986,** *25*, 3765−3770. (b) Braunstein, P.; Matt, D.; Nobel, D.; Fischer, J. *J. Chem. Soc., Chem. Commun.* **1987**, 1530−1532. (c) Braunstein, P.; Matt, D.; Nobel, D.; Balegroune, F.; Bouaoud, S.-E.; Grandjean, D.; Fischer, J. *J. Chem. Soc., Dalton Trans.* **1988**, 353−361. (d) Balegroune, F.; Braunstein, P.; Grandjean, D.; Matt, D.; Nobel, D. *Inorg. Chem.* **1988,** *27*, 3320−3325.

(8) (a) Klabunde, U.; Mulhaupt, R.; Herskovitz, T; Janowicz, A. H; Calabrese, J.; Ittel, S. D. *J. Polym. Sci.* **1987**, *25*, 1989−2003. (b) Klabunde, U.; Ittel, S. D. *J. Mol. Catal.* **1987**, *41*, 123−134.

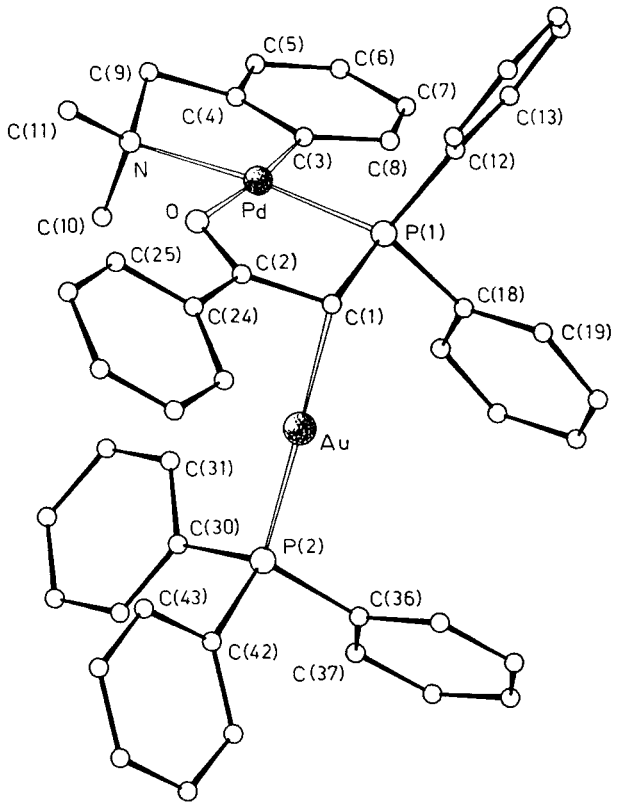

Figure 1. Crystal structure of complex [(dmba)Pd{$Ph_2PCH(AuPPh_3)$-C(O)Ph}](BF_4) in **4a**·$^1/_2C_7H_8$. The hydrogen atoms are not shown, including that at C(1).

Table 1. Selected Bond Distances (Å) and Angles (deg) for Complex **4a**

Au−P(2)	2.272(2)	Au−C(1)	2.146(6)
Pd−P(1)	2.234(2)	Pd−O	2.128(5)
Pd−N	2.127(5)	Pd−C(3)	1.990(7)
P(1)−C(1)	1.817(7)	O−C(2)	1.260(7)
N−C(9)	1.481(15)	C(1)−C(2)	1.435(6)
C(4)−C(9)	1.493(12)		
P(2)−Au−C(1)	178.9(2)	N−Pd−C(3)	83.1(2)
O−Pd−N	91.8(2)	P(1)−Pd−C(3)	102.7(2)
P(1)−Pd−O	82.5(1)	Pd−P(1)−C(1)	99.3(2)
Pd−O−C(2)	118.0(4)	Pd−N−C(9)	106.1(5)
Au−C(1)−P(1)	104.7(3)	P(1)−C(1)−C(2)	111.9(4)
Au−C(1)−C(2)	99.1(4)	O−C(2)−C(1)	122.3(5)
C(1)−C(2)−C(24)	121.3(5)	O−C(2)−C(24)	116.4(5)
Pd−C(3)−C(8)	131.0(5)	Pd−C(3)−C(4)	112.2(5)
C(3)−C(4)−C(9)	117.7(8)	C(3)−C(4)−C(5)	120.3(7)
C(5)−C(4)−C(9)	120.8(8)	C(3)−C(8)−C(7)	120.8(6)
N−C(9)−C(4)	108.4(7)		

before.[6] The structure drawn for complexes **4** has now been confirmed by an X-ray diffraction study on **4a**.

Crystal Structure of the Pd(II)−Au(I) Complex 4a·$^1/_2C_7H_8$. A view of the molecular structure of this complex is show in Figure 1, selected distances and angles are given in Table 1. The palladium atom has a square planar coordination involving the N and C(3) atoms of the chelating cyclometalated dmba ligand and the P(1) and O atoms of the chelating phosphino enolate ligand, the C(3) atom being trans with respect to the O atom. The coordinated N, C(3), P(1) and O atoms deviate from the mean plane through them by 0.105(5), −0.037(7), 0.009(2), and −0.017(4) Å, respectively, with the Pd atom out of this plane by −0.014(2) Å. The bond distances to Pd are in the normal range. The Pd−O distance of 2.128(5) Å is slightly longer than in [*cis*-Pd{$Ph_2PCH_2C(O)Ph$}$_2$][BF_4][B_2F_7] (2.102(4) Å),[9] probably as a result of the high *trans influence* of the *σ*-bonded carbon C(3). The dimensions within the dmba chelate are similar to those found for this ligand in other Pd(II) complexes.[10] Both chelating ligands form five-membered rings with the metal atom, and the N−Pd−C(3) and O−Pd−P(1) bite angles are 83.1(2) and 82.5(1)° respectively. These five-membered rings have an envelope conformation with C(9) being 0.422(12) Å out of the mean plane passing through the Pd, C(3), C(4), and N atoms, and the Pd atom being 0.591(2) Å out of the mean plane through the P(1), C(1), C(2), and O atoms. Because of the addition of the Au(PPh_3) group on C(1), which becomes sp^3 hybridized, the values of the C(1)−C(2) and C(2)−O bond distances, 1.435(6) and 1.260(7) Å, show, as expected, a greater double bond character for the C−O bond than in phosphino enolate−palladium complexes (see also below the structure of **5b**).[3a,4a,7d] The Au atom is almost linearly coordinated by C(1) and P(2) [Au−C(1) = 2.146(6) Å and Au−P(2) = 2.272(2) Å, C(1)−Au−P(2) = 178.9(2)°]. The value of the Au−C bond length is comparable to that found, 2.128(21) Å,[11] in [Au_2{μ-[$CH(PPh_3)$]$_2$CO}][ClO_4]$_2$, in which the Au atom is also bound to a sp^3-hybridized carbon atom adjacent to a PPh_3 and a CO group.

Synthesis, Structure, and Magnetism of Heterobinuclear Ni(II)−Co(II) Complexes. The reaction of complexes **1a−c** with 1 equiv of anhydrous cobalt(II) iodide in Et_2O afforded the air-stable adducts *cis*-[Ni{R'_2PCH···C(···O)R}$_2$]CoI_2 (**5a**, R = Ph; **5b**, R = *p*-C_6H_4Me; **5c**, R = Me) in good yield (eq 5). In contrast to the reactions described in eqs 2 and 3, no

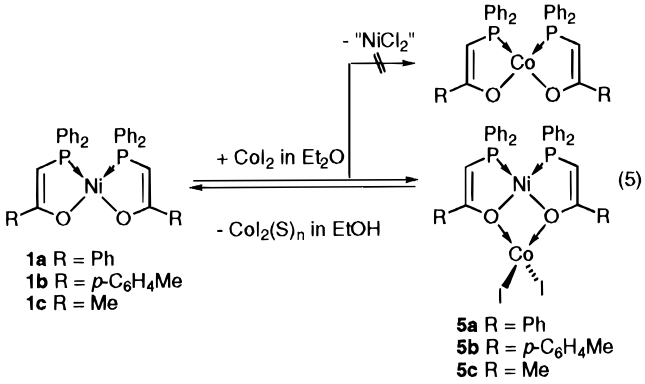

transmetalation was observed in this reaction. This should be related to prior unsuccessful attempts to prepare a Co(II) bis(phosphino enolate) complex: octahedral *fac*- or *mer*-tris(phosphino enolate)−Co(III) complexes were isolated instead.[12]

The IR spectrum of **5a−c** exhibits typical absorptions between 1568 and 1505 cm^{-1} associated with the [ν(C···C) + ν(C···O)] vibrations of the phosphino enolate ligand. This was taken as a strong indication that complexes **1a−c** were acting as chelating, oxygen donor metalloligands toward the CoI_2 unit. An X-ray diffraction study was carried out on **5b** (see below) in order to firmly establish the detailed structure of these complexes. The bis(phosphino enolato)nickel complex acts as a four-electron donor *O,O* chelate and the phosphino

(9) Braunstein, P.; Douce, L.; Fischer, J.; Craig, N. C.; Goetz-Grandmont, G.; Matt, D. *Inorg. Chim. Acta* **1992**, *194*, 151−156.
(10) (a) Braunstein, P.; Matt, D.; Nobel, D.; Bouaoud, S.-E.; Grandjean, D. *J. Organomet. Chem.* **1986**, *301*, 401−410. (b) Canty, A. J. In *Comprehensive Organometallic Chemistry*, 2nd ed.; Abel, E. W.; Stone, F. G. A.; Wilkinson, G., Eds.; Pergamon: Oxford, England, 1995; Vol. 9, Chapter 5, pp 1−72.
(11) Vicente, J.; Chicote, M.-T.; Saura-Llamas, I.; Jones, P. G.; Meyer-Bäse, K.; Erdbrügger, C. F. *Organometallics* **1988**, *7*, 997−1006.
(12) Braunstein, P.; Kelly, D. G.; Tiripicchio, A.; Ugozzoli, F. *Inorg. Chem.* **1993**, *32*, 4845−4852.

enolate ligand as a chelating−bridging μ-$\eta^1(O)$:$\eta^2(P,O)$, five-electron donor ligand. These heterobinuclear complexes appear to be the first examples where a phosphino enolate oxygen atom bridges between two different transition metal atoms. We have previously reported a related coordination mode in a Ru_3 cluster.[13] The present situation is however reminiscent of the bonding found in recent phosphinophenolate complexes.[14] Although numerous dinuclear complexes, with or without a metal-metal bond, are known which contain a bridging alkoxy, hydroxy or phenoxy oxygen,[15−17] no Ni(II)−Co(II) complex containing a bridging oxygen function appears to have been described, with the exception of those already mentioned.[14] However, bridging oxygen donor atoms are often found in coordination complexes of more oxophilic metals, e.g. in organolithium or -magnesium chemistry.[18]

The oxygen−cobalt dative bond is maintained in CH_2Cl_2 solution but it is labile in donor solvents such as EtOH, acetonitrile or THF, where the precursors complexes **1a**−**c** were regenerated and could be separated from $CoI_2(solvent)_n$ by precipitation with EtOH (eq 5).

In contrast to the situation with **1a**, no reaction was observed between **5a** and an activated alkyne such as $MeO_2C{-}C{\equiv}C{-}CO_2Me$. Obviously, the coordination of the metal electrophile CoI_2 has significantly decreased the nucleophilic character of the *P*,*O* chelate compared with its precursor complex **1a**.[4]

Attempts to form other bimetallic complexes by coordination of **1a** to other electrophilic metal complexes than CoI_2, such as anhydrous $CoCl_2$, MnI_2, $NiBr_2$, $NiCl_2(Py)_4$, or $[Ni(NCMe)_6][BF_4]_2$, have so far been unsuccessful.

Crystal Structure of the Ni(II)−Co(II) Complex 5b·CH_2Cl_2. The crystal structure consists of discrete monomeric molecular units separated by normal van der Waals contacts and dichloromethane molecules of solvation. The molecular structure of the complex is shown in Figure 2, and selected bond lengths and angles are listed in Table 2. The planar coordination geometry around the nickel atom is defined by the two P and two O atoms of the two phosphino enolate ligands which are in a mutual cis arrangement. The two *P*,*O* ligands have almost identical geometries, bond lengths and angles. The five atoms Ni, P(1), P(2), O(1), and O(2) are coplanar (distances from the mean plane <0.05 Å) and the C(1), C(2), C(3), and C(4) carbon atoms are, in first approximation, in this plane (distances <0.2 Å) but the Co atom is out of this plane by 1.058(1) Å. The two Ni−P and the two Ni−O bond length values are respectively 2.143(2), 2.156(2) Å and 1.932(5), 1.910(5) Å. The bridging oxygen atoms O(1) and O(2) act as 2 electron donors toward the Co atom. The coordination around the Co atom is pseudotetrahedral, with an angle of 88.4(1)° between the planes formed by Co, I(1), I(2) and Co, O(1), O(2). The NiO(1)O(2)Co unit is bent along the axis joining the oxygen atoms, generating a dihedral angle of 148° between the NiO(1)O(2) and CoO(1)O(2) planes. The oxygen atoms O(1) and O(2) are out of the planes (0.372(5), 0.388(5) Å) formed by Ni, Co, C(4) and Ni, Co, C(1), respectively, and the angles Ni−O(1)−C(4) and Ni−O(2)−C(1) (118.2(5)°, 117.6(5)°) are smaller than Co−O(1)−C(4), and Co−O(2)−C(1) (134.4(5), 132.6(5)°). This arrangement renders the enolate C···C···O system prochiral. This contrasts with homobinuclear Co(II)−Co(II) complexes containing a bridging phenoxy oxygen, where the $Co(1)O_2Co(2)$ network is planar.[14] As for the Ni coordination, the two chelating, bridging ligands introduce a strong distorsion of the O−Co−O angle (78.1(2)°) which is accompanied by high values for the I(1)−Co−O(1) and I(2)−Co−O(2) angles (122.2(1), 119.5(2)°). The bond lengths C(1)−C(2) (1.34(1) Å), C(3)−C(4) (1.35(1) Å), and C(1)−O(2), C(4)−O(1) (1.34(1) Å) of the enolate moiety are comparable with and similar to those in **1a**,[19] which is indicative of electron delocalization within the system. The coordination of the cobalt(II) atom leads to a lengthening of the Ni−O distances (1.910(5) and 1.932(5) Å

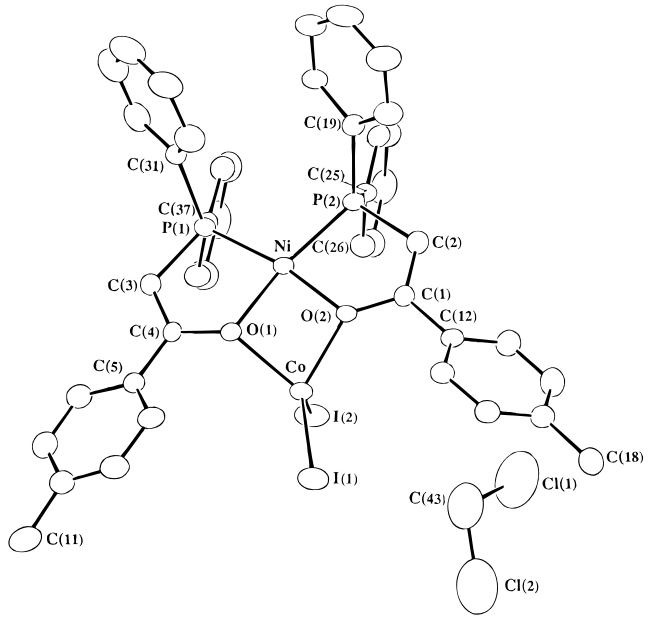

Figure 2. Crystal structure of *cis*-[Ni{$Ph_2PCH{\cdot\cdot}C({\cdot\cdot}O)$(*p*-$C_6H_4CH_3$}$_2$]$CoI_2{\cdot}CH_2Cl_2$ (**5b**·CH_2Cl_2).

Table 2. Selected Bond Distances (Å) and Angles (deg) for **5b**·CH_2Cl_2[a]

Co−I(1)	2.545(1)	O(1)−O(2)	2.553(7)
Co−I(2)	2.553(1)	O(1)−C(4)	1.34(1)
Co−O(1)	2.036(5)	O(2)−C(1)	1.34(1)
Co−O(2)	2.016(5)	C(1)−C(2)	1.34(1)
Ni−P(1)	2.143(2)	C(3)−C(4)	1.35(1)
Ni−P(2)	2.156(2)	P(1)−C(31)	1.808(8)
Ni−O(1)	1.932(5)	P(1)−C(37)	1.813(9)
Ni−O(2)	1.910(5)	P(2)−C(19)	1.808(8)
P(1)−C(3)	1.769(8)	P(2)−C(25)	1.815(9)
P(2)−C(2)	1.780(9)		
I(1)−Co−I(2)	116.36(5)	Ni−P(1)−C(3)	98.0(3)
I(1)−Co−O(1)	122.2(1)	Ni−P(2)−C(2)	97.7(3)
I(1)−Co−O(2)	119.5(2)	Ni−O(1)−C(4)	118.2(5)
I(2)−Co−O(1)	106.4(1)	Ni−O(2)−C(1)	117.6(5)
I(2)−Co−O(2)	107.9(2)	Co−O(1)−Ni	91.3(2)
O(1)−Co−O(2)	78.1(2)	Co−O(2)−Ni	92.5(2)
P(1)−Ni−P(2)	100.54(9)	Co−O(1)−C(4)	134.4(5)
P(1)−Ni−O(1)	87.9(2)	Co−O(2)−C(1)	132.6(5)
P(1)−Ni−O(2)	170.0(2)	P(1)−C(3)−C(4)	116.5(6)
P(2)−Ni−O(1)	171.1(2)	P(2)−C(2)−C(1)	115.2(7)
P(2)−Ni−O(2)	88.1(2)	O(1)−C(4)−C(3)	119.4(7)
O(1)−Ni−O(2)	83.3(2)	O(2)−C(1)−C(2)	121.0(7)

[a] Numbers in parentheses are estimated standard deviations in the least significant digits.

(13) Braunstein, P.; Coco Cea, S.; Bruce, M. I.; Skelton, B. W.; White, A. H. *J. Organomet. Chem.* **1992**, *423*, C38−C42.
(14) (a) Dunbar, K. R. *Comments Inorg. Chem.* **1992**, *13*, 313−357. (b) Dunbar, K. R.; Quillevéré, A. *Organometallics* **1993**, *12*, 618−620.
(15) Chang, Y.; Chen, Q.; Khan, M. I.; Salta, J.; Zubieta, J. *J. Chem. Soc., Chem. Commun.* **1993**, 1872−1874.
(16) Lachicotte, R.; Kitaygorodskiy, A.; Hagen, K. S. *J. Am. Chem. Soc.* **1993**, *115*, 8883−8884.
(17) (a) Nanda, K. K.; Thompson, L. K.; Bridson, J. N.; Nag, K. *J. Chem. Soc., Chem. Commun.* **1994**, 1337−1338. (b) Jeffery, J. C.; Thornton, P.; Ward, M. D. *Inorg. Chem.* **1994**, *33*, 3612−3615. (c) Krebs, B.; Schepers, K.; Bremer, B.; Henkel, G.; Müller-Warmuth, W.; Griesar, K.; Haase, W. *Inorg. Chem.* **1994**, *33*, 1907−1914.
(18) (a) Seebach, D.; Amstutz, R.; Laube, T.; Schweizer, W. B.; Dunitz, J. D. *J. Am. Chem. Soc.* **1985**, *107*, 5403−5409. (b) Williard, P. G.; Salvino, J. *J. Chem. Soc., Chem. Commun.* **1986**, 153−154.
(19) Qichen, H.; Minzhi, X.; Yanlong, Q.; Weihua, X.; Meicheng, S.; Youqi, T. *J. Organomet. Chem.* **1985**, *287*, 419−426.

in **5b** vs 1.857(14) and 1.877(11) Å in **1a**) and to the closing of the O(1)−Ni−O(2) angle from 86.9° in **1a** to 83.3(2)°. This is compensated by the high value of the opposite angle P(1)−Ni−P(2) (100.54(9)°). The molecular conformation of the phenyl groups of the phosphines is governed by a face to face arrangement with van der Waals interactions. The mean distance between the two pseudoparallel (16.8°) planes C(25)···C(30) and C(37)···C(42) is 3.35 Å and that between the two planes (5.5°) C(19)···C(24) and C(31)···C(36) is 3.36 Å. The tolyl planes have nearly the same orientation (29.1(4)°, 20.7(5)°) with respect to the Ni, P(1), P(2), O(1), O(2) plane.

Isomerization Reactions of the α-Phosphino Enolate Ni(II) Complexes by Coordination to CoI_2. The bis(phosphino enolate) complexes of Ni(II) can adopt a *trans*-arrangement of the phosphorus atoms when bulky substituents are present on phosphorus. For example, in *trans*-[Ni{R′$_2$PCH···C(···O)R}$_2$] (R = Ph, ^{t}Bu) only the *trans* isomer was observed for R′ = ^{t}Bu.[20] However, with R′ = ^{i}Pr, we have observed the formation of a mixture of the *cis*- and *trans*-isomers of [Ni{^{i}Pr$_2$PCH···C(···O)Ph}$_2$] (**6**) in a *ca.* 1:1 ratio determined by integration of the ^{1}H NMR PCH signals and of the ^{31}P{^{1}H} NMR resonances (eq 6). Isomers *trans*-**6** and *cis*-**6** were

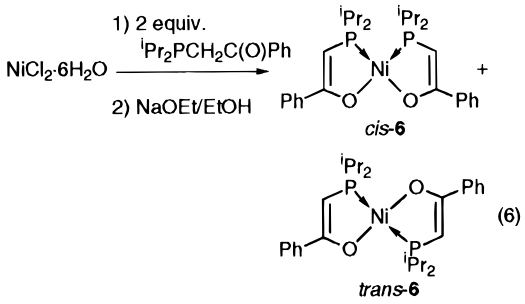

characterized by a singlet in the ^{31}P{^{1}H} NMR spectrum, at δ 50.0 and 39.3, respectively. The broad signals in ^{1}H NMR at δ 4.37 and 4.19 corresponding to the PCH proton could not be assigned to a given isomer. The IR spectrum (KBr pellet) of *trans*-**6** and *cis*-**6** shows only one absorption band at 1517 cm^{-1} for the [ν(C···C) + ν(C···O)] vibration. The formation of both *cis*- and *trans*-**6** can be explained by two opposite effects: the steric effect favors the *trans*-arrangement while the electronic effect favors the *cis*-arrangement (*trans*-influence of the donor atoms). The fact that these isomers were always present in solution suggested the existence of an equilibrium (see below). We then studied the coordination properties of **6** toward CoI_2.

Under the conditions described for complexes **1a**−**c**, the reaction of **6** with anhydrous CoI_2 led to the heterobinuclear complex *cis*-[Ni{^{i}Pr$_2$PCH···C(···O)Ph}$_2$]CoI_2 (**7**) in 76% yield (Scheme 2). The ^{31}P{^{1}H} NMR spectrum of the reaction mixture showed only the presence of complex **7**. The disappearence of *trans*-**6** therefore confirms that both isomers were in equilibrium in solution and that coordination of CoI_2 completely shifted the equilibrium toward the formation of **7**. When **7** was dissolved in donor solvents such as THF, the ^{31}P{^{1}H} NMR spectrum showed only one signal at δ 39.3 which corresponds to *cis*-**6** (Scheme 2) which is therefore the kinetic isomer. Unfortunately, *cis*-**6** and the $CoI_2(S)_n$ formed could not be separated due to similar solubility properties and to the progressive transformation of *cis*-**6** in the reaction mixture. Thus,

(20) Moulton, C. J.; Shaw, B. L. *J. Chem. Soc., Dalton Trans.* **1980**, 299−301.

Scheme 2

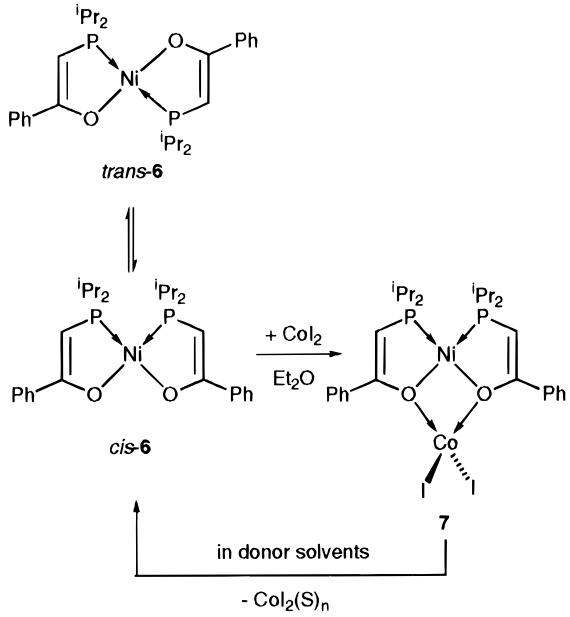

^{31}P{^{1}H} NMR monitoring showed a decrease of the intensity of the singlet at δ 39.3, which was progressively replaced by an AB pattern at δ 57.4 and 29.8 with a ^2J(PP) of 304 Hz. This is typical for a trans arrangement of chemically different P atoms. It is interesting to note that this transformation has not been observed with complexes **5**, which contain a PPh_2 group in place of the more electron donor P^{i}Pr$_2$ substituent. In order to shed some light on this transformation, we exposed complex **7** to different solvents (THF, acetonitrile) and iodine-containing reagents, such as [NMe_4]I and I_2. Only in the latter case was a similar behavior observed. We therefore suggest that some I_2 is liberated by decomposition that would oxidize *cis*-**6** to form a square-planar Ni(II) complex. In view of independent observations that iodine can indeed react with metal-coordinated phosphino enolate complexes to form complexes containing the new ligand $Ph_2PCH(I)C(O)Ph$,[5b] we suggest in the present case the formation of *trans*-[Ni(I){^{i}Pr$_2$PCH···C(···O)Ph}{^{i}Pr$_2$PCH(I)C(O)Ph}]. This is also consistent with the observation in the ^{1}H NMR spectrum of two resonances at δ 4.30 and 3.56 for the CH protons.

In view of the donor character of the enolate oxygen atoms in complexes **5** and **6** and of the possible use of Lewis acidic alkylating agents such as $AlMe_3$ to transform **1a** into an active olefin polymerization catalyst,[8] we examined the reaction between the SHOP-type catalyst [Ni(Ph){Ph_2PCH···C(···O)Ph}(PPh_3)][1] and CoI_2. Under the conditions used for the synthesis of complexes **5** or **7**, but using only 0.5 equiv CoI_2, we obtained after extraction with CH_2Cl_2 a green solid. The reaction was not complete, and a pure complex could not be isolated. However, a new paramagnetic complex had formed, as indicated by ^{1}H and ^{31}P{^{1}H} NMR spectroscopy: ^{1}H chemical shifts are observed in the range 29.6 to −37.2 ppm and a signal at −96.5 ppm is found in ^{31}P{^{1}H} NMR. A greater lability or instability of this complex compared to **5** or **7** would obviously result from the lack of chelating effect.

NMR Spectroscopic Studies of Paramagnetic Complexes 5b. The magnetic properties of heteropolymetallic systems containing bridging atoms or groups are of interest for biologists and bioinorganic chemists investigating the structure and the role of polymetallic active sites in biological processes, and for physicists and physical inorganic chemists who study new magnetic materials. It has generally been found that the overall

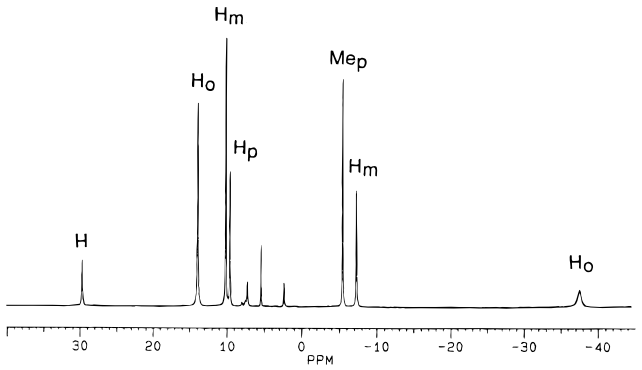

Figure 3. ^{1}H NMR spectrum of **5b** in CD_2Cl_2 at 298 K.

Table 3. ^{1}H NMR Data (at 298 K, in CD_2Cl_2) for **5b**[a]

	enolate	$P(C_6H_5)_2$			$-C_6H_4Me$		
	(a) H	(b) $H_{o\,or\,m}$	(c) $H_{m\,or\,o}$	(d) H_p	(e) Me_p	(f) H_m	(g) H_o
δ (ppm)	30.04	14.16	10.17	9.56	−5.88	−8.04	−39.53

[a] Other peaks at δ 7.20, 5.32, and 2.29 were attributed to crystallization solvents.

properties are not just the sum of the magnetic properties of each individual ion, but rather they result from both the nature and the magnitude of the interactions between the metal ions within the molecular unit.[21]

In complex **5b**, the presence of the paramagnetic center leads in ^{1}H NMR spectroscopy to chemical shifts in the range δ −39.5 to 30.0 ppm at room temperature (Figure 3). This also explains the $^{31}P\{^1H\}$ NMR spectrum of **5b** which exhibits a singlet at −102.5 ppm. However, complex **5b** does not exhibit any EPR signal even when cooled down to 40 K. The availability of NMR spectra for the paramagnetic species suggests that the unpaired electron is rather localized on the cobalt(II) atom and not fully delocalized over the *P,O* ligands. As shown by the crystal structure of complex **5b** (Figure 2), the bridging oxygen atom of the *P,O* chelate has a pyramidal environment. This arrangement could lead to a weak overlap of magnetic orbitals as well as to some electron delocalization between the two metal centers. The ^{1}H NMR spectrum shows four well-resolved downfield signals (a−d) in addition to three other more upfield shifted (e−g), as shown in Figure 3. The assignment of these signals given in Table 3 was confirmed by their respective intensities and by analogy with the ^{1}H NMR spectra of **5a** and **5c**. The presence of a paramagnetic center leads to a very different chemical shift for the aromatic protons of the $-C_6H_5$ (**5a**) and the *ortho*-and *meta* protons of the C_6H_4Me (**5b**) groups. A similar observation has previously been made in a heterobinuclear Fe(II)−Co(II) complex containing a bridging phenolate.[22a] The chemical shift of the enolate proton (a) indicates some delocalization of the unpaired electron between the bridging enolate and the cobalt(II) atom. The broad peak assigned to the *ortho* proton (g) could be due to through-space dipolar interaction with the near cobalt(II), as found in mononuclear Co(II) complexes.[22b]

We then investigated the variable-temperature ^{1}H NMR spectrum of **5a**, in the range +25 °C [$1/T = 3.35 \times 10^{-3}$ (K^{-1})] to −35 °C [4.20×10^{-3} (K^{-1})] (Figure 4). When the temperature decreased, all signals were shifted and an accentuation of the chemical shifts was observed, which was a consequence of the total magnetic susceptibilty (χ_m) variation.

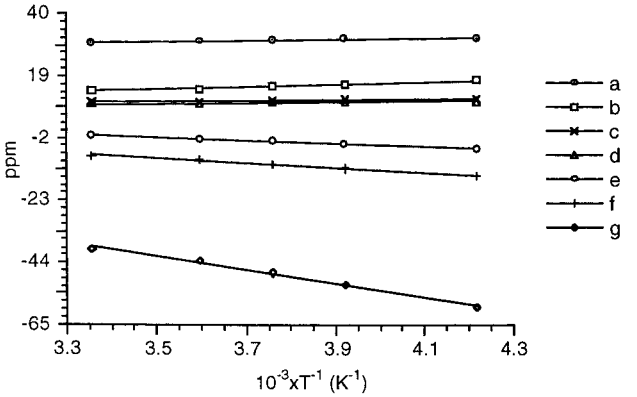

Figure 4. Experimental curves of **5a** (in CD_2Cl_2) [δ_i (ppm) = $f(1/T)$].

Table 4. Variable-Temperature ^{1}H NMR Spectrum of **5a** in CD_2Cl_2

	enolate	$-P(C_6H_5)_2$			$-C-C_6H_5$		
T (K)	(a) H	(b) $H_{o\,or\,m}$	(c) $H_{m\,or\,o}$	(d) H_p	(e) H_p	(f) H_m	(g) H_o
298	30.35	14.14	10.17	9.54	−1.36	−8.01	−39.48
278	30.99	14.88	10.47	9.77	−2.22	−9.39	−43.55
266	31.39	15.58	10.76	9.98	−3.05	−10.71	−47.41
255	31.67	16.35	11.07	10.21	−3.98	−12.17	−51.68
237	31.91	17.69	11.60	10.63	−5.63	−14.69	−59.05

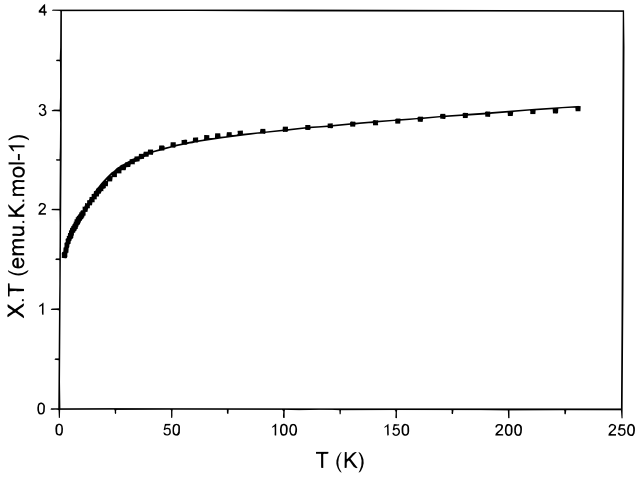

Figure 5. Temperature dependence of the χT product for complex **5c**. The full line represents the theoretical curve for isolated cobalt(II) centers.

In a magnetic field, a heterobinuclear complex of type **5** will exhibit two different magnetic moments: the induced moment of the diamagnetic fragment **1** which is opposed by the magnetic moment of the paramagnetic Co(II) fragment. When the temperature decreases, the paramagnetism cancels more and more the diamagnetism, and leads to the accentuation of the chemical shifts observed on the ^{1}H NMR spectrum of **5a**. These experimental curves show that the chemical shift of the *ortho* proton (g) is the most affected (Table 4). This observation suggests that the influence of the paramagnetic center is more important through space than through the enolate bridge. This is confirmed when the phenyl group (containing the protons e−g) in complex **5a** is replaced by a methyl substituent which has a chemical shift at δ −83.8 ppm in **5c**.

Magnetic Properties of the Ni−Co Complexes. The temperature-dependent magnetic behavior of the above compounds have been measured by means of a SQUID magnetometer (Métronique) and a DSM8 susceptometer (Manics), in the temperature range 2−300 K and applied fields 0−20 kOe. Compounds **5a,c** and **7** show a similar behavior, illustrated in Figure 5 for **5c**. The χT product decreases regularly from room temperature down to 50 K, then more sharply upon cooling toward a non-zero value (∼1.5 emu·K·mol^{-1}) for T = 2 K. In

(21) (a) Kahn, O. *Struct. Bonding* **1987**, *68*, 89−167. (b) Kahn, O. *Molecular Magnetism*; VCH: Weinheim, Germany, 1994.
(22) (a) Wang, Z.; Holman, T. R.; Que, J.; Jr. *Magn. Reson. Chem.* **1993**, *31*, S78−S84. (b) Moratal, J. M.; Salgado, J.; Donaire, A.; Jiménez, H. R.; Castelles, J. *Inorg. Chem.* **1993**, *32*, 3587−3588.

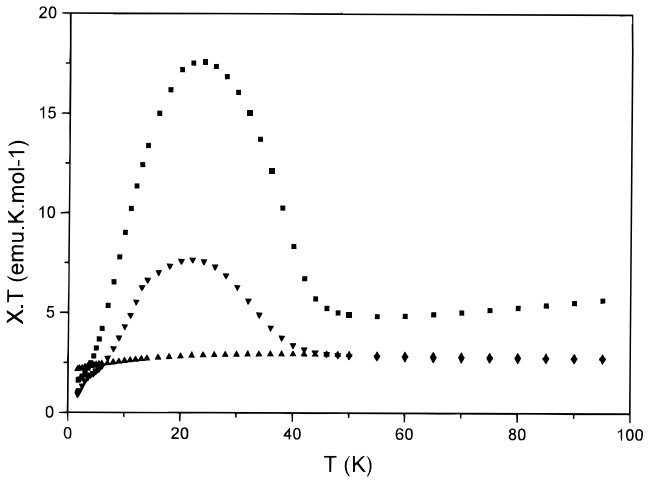

Figure 6. Temperature dependence of the χT product for complex **5b**. The different variations show the influence of sample aging.

turn, compound **5b** exhibits a different χT variation (Figure 6), since a large bump is observed around 30 K, the height of which depends on the sample aging. Magnetization measurements, performed at different temperatures up to 300 K, show that a ferromagnetic component is superimposed to the classical linear variation, due likely to the presence of a small amount of metal impurity. Assuming that cobalt metal particles are responsible for this behavior (considering the stability of the precursors **1** and the lability of the O→Co dative bonds), we obtain from the magnetization results an estimate of 0.02% of metal impurity.

The behavior observed for the other compounds could be the signature of magnetic exchange interactions between the metal ions. In fact, nickel(II) in square planar geometry is nonmagnetic, so that the results can only be explained by considering cobalt(II) ions in distorted tetrahedral surrounding. Previous work reported in the literature shows that a zero-field splitting of the $^4A_2$ ground-term generally occurs for cobalt(II) in such an environment, which is usually rather large.[23−26] This splitting (D)[27] is related to the energy of the excited configurations ^4E and $^4B_2$, giving the effective doublets $S^z = |\pm^1/_2\rangle$ or $S^z = |\pm^3/_2\rangle$ as low-lying spin states, and thus inducing a temperature-dependent magnetic moment. In Cs_2CoCl_4,[23] the zero-field splitting stabilizes the $|\pm^1/_2\rangle$ state, while in Cs_3CoCl_5 [24] the $|\pm^3/_2\rangle$ state is lower. In both cases, the magnetic susceptibility, given in the Appendix, depends strongly on D at low temperature (for $kT/D < 1$). This model allows a very good description of the $\chi T = f(T)$ data for compound **5c** (Figure 5), using the parameters $D = 39.9$ K, which stabilizes the spin doublet $|\pm^1/_2\rangle$, $g_{\parallel} = 2.72$, $g_{\perp} = 2.34$, and $\chi_{vv} = 1.52 \times 10^{-3}$ emu/mol.

Correlations between structural findings and magnetic properties have been reported for the $CoCl_4^{2-}$ ion in close-packed lattices.[23−25] It has been shown, in particular, that zero-field splitting is typically on the order of 10−20 K, and that a change in sign of D occurs for a Cl−Co−Cl angle close to 109.50°. Thus, for Cs_3CoCl_5, characterized by bond angles ranging between 107.2 and 110.6°, D is negative while it is positive for Cs_2CoCl_4 exhibiting more distorted $CoCl_4^{2-}$ units. A direct comparison of our results with those of $CoO_2I_2^{4-}$ species is tricky, due to the presence of two I^- ligands in the coordination sphere of the metal ion. Indeed, the bond lengths differ drastically, since they range from 2.016, 2.036 Å (Co−O bonds) to 2.545, 2.553 Å (Co−I bonds), while in the chlorides they are of the order of 2.25 Å. Furthermore, the O−Co−O bond angle is very small (∼78°) while the I−Co−I counter-angle is large (∼116°) compared with the bond angles of symmetrical units. As a result, the local symmetry is lowered to C_{2v}, promoting a large zero-field splitting which allows to explain the magnetic properties in the frame of a molecular model.

Discussion

The reaction of *cis*-[Ni{$Ph_2PCH\cdots C(\cdots O)Ph$}$_2$] (**1**) with $PtCl_2$(COD) has yielded *cis*-[Pt{$Ph_2PCH\cdots C(\cdots O)Ph$}$_2$] (**3**) as a result of a transmetalation reaction of the anionic *P*,*O* chelate which may be initiated by nucleophilic attack of the enolate carbon onto the other metal center. This observation suggests that the reaction is under thermodynamic control; bonds to platinum are generally more stable than to nickel. This is consistent with the reactivity trends of *cis*-[M{$Ph_2PCH\cdots C(\cdots O)Ph$}$_2$] (M = Ni > Pd > Pt) toward activated alkynes which occurred by carbon(enolate)−carbon coupling and metal−oxygen bond dissociation and were complete after 12 h for M = Ni and 72 h for M = Pt.[4] In a similar way, the enolate moiety of [(dmba)Pd{$Ph_2PCH\cdots C(\cdots O)Ph$}] behaves as a *C*-nucleophile toward [(C N)Pd(μ-Cl)]$_2$ or [Au(PPh_3)]$^+$, affording in the latter case complex **4a** which was structurally characterized. However, the reactions between *cis*-[Ni{$R'_2PCH\cdots C(\cdots O)R$}$_2$] and anhydrous CoI_2 afforded the heterobinuclear Ni-Co complexes **5a**−**c** and **7** in which the nickel complex acts as a 4 electron donor toward the cobalt ion. It is interesting that the chelating behavior of **1a** via its oxygen atoms has been previously observed in its reaction with $AlMe_3$ which afforded the ethylene polymerization catalyst formulated as **A**.[8] The

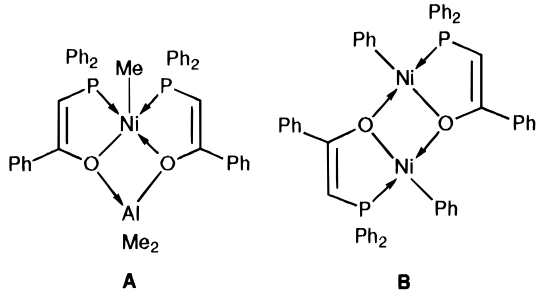

SHOP-type catalyst [Ni(Ph){$Ph_2PCH\cdots C(\cdots O)Ph$}($PPh_3$)] was also shown to behave as an oxygen-donor metalloligand toward CoI_2. A reasonable structural formulation for this trinuclear complex would be that of a tetrahedral Co(II) complex containing two monodentatate oxygen-donor nickel complex molecules as in CoI_2[Ni(Ph){$Ph_2PCH\cdots C(\cdots O)Ph$}-($PPh_3$)]$_2$. The ability of the oxygen atom in [Ni(Ph){Ph_2-

(23) McElearney, J. N.; Merchant, S.; Shankle, G. E.; Carlin, R. L. *J. Chem. Phys.* **1977**, *66*, 450.
(24) Wielinga, R. F.; Blöte, H. W. J.; Roest J. W.; Huiskamp, W. J. *Physica* **1967**, *34*, 223.
(25) Algra, H. A.; de Jongh, L. J.; Blöte, H. W. J.; Huiskamp, W. J.; Carlin, R. L. *Physica* **1976**, *B82*, 239.
(26) McElearney, J. N.; Shankle, G. E.; Schwartz, R. W.; Carlin, R. L. *J. Chem. Phys.* **1972**, *56*, 3755.
(27) We define as D the splitting of the $^4A_2$ ground term resulting from the mixing with the $^4B_2$ and ^4E excited configurations. The susceptibilities parallel and perpendicular to the z axis are then given by

$$\chi_z = Ng^2\mu_B{}^2/4kT(1 + 9\exp(-D/kT))/(1 + \exp(-D/kT)) + \chi_0$$

$$\chi_x = Ng^2\mu_B{}^2/kT(1 + \exp(-D/kT))^{-1} + 3Ng^2\mu_B{}^2\tanh(D/2kT)/2D + \chi_1$$

where χ_0 and χ_1 are second-order Zeeman contributions related to the excited states $^4B_2$ and ^4E, respectively. The average susceptibility is deduced from $\chi = {}^1/_3(\chi_z + 2\chi_x)$.

PCH···C(···O)Ph}(PPh$_3$)] to donate an unused electron pair to an unsaturated metal center has been previously observed in the homodinuclear complex [Ni(Ph){Ph$_2$PCH···C(···O)Ph}]$_2$ (**B**), which forms in the absence of an external donor ligand.[8] These addition reactions show the significant *O*-basicity of the *P,O* chelate in its metal complexes. Obviously, the control of the chemospecificity of the coordinated ligand [Ph$_2$PCH···C(···O)Ph]$^-$ toward metal electrophiles depends upon the nature of both the metal complex containing the *P,O* chelate and the metal electrophile, which may allow a fine-tuning of stoichiometric or catalytic reactivity.

The reversible coordination of CoI_2 in the Ni(II)−Co(II) heterobinuclear species **5** leads to the possibility of isomerizing the α-phosphino enolate nickel(II) complexes from the *trans*- to the *cis*-isomer. In the case of complex **7**, dissociation in donor solvents with liberation of *cis*-**6** and progressive decomposition led to a byproduct formulated as *trans*-[Ni(I){^{i}Pr$_2$PCH···C(···O)Ph}{^{i}Pr$_2$PCH(I)C(O)Ph}]. The magnetic properties of the paramagnetic Ni−Co bimetallic complexes **5** have been presented and discussed above. They could be explained by a molecular model involving distorted Co(II) d^7 centers, without invoking intermolecular interactions. The latter also appeared unlikely in view of the packing in the solid state and the similar behavior of complexes **5a**−**c**, indicating that the phenyl, *p*-tolyl, or methyl substituent, respectively, does not provide communication between the isolated molecules. However, the slight structural modifications that may result from this replacement could certainly influence slightly the coordination geometry about the Co(II) center—in particular the value of the O(1)−Co−O(2) angle—and therefore explain magnetic differences within this family of complexes. This will require further structural/magnetic investigations.

Experimental Section

Reagents and Physical Measurements. All reactions were performed in Schlenk-type flasks under nitrogen. Solvents were purified and dried under nitrogen by conventional methods. The ^{1}H and ^{31}P{^{1}H} NMR spectra were recorded at 300.13 and 121.5 MHz, respectively, on a FT Bruker AC 300 instrument. IR spectra were recorded in the 4000−400-cm^{-1} range on a Bruker IFS66 FT spectrometer.

Syntheses. The ligands Ph$_2$PCH$_2$C(O)Ph and ^{i}Pr$_2$PCH$_2$C(O)Ph and the complexes [PtCl$_2$(COD)], *cis*-[M{Ph$_2$PCH···C(···O)Ph}$_2$] (**1a**, M = Ni; **3**, M = Pt), *cis*-[Ni{Ph$_2$PCH···C(···O)Me}$_2$] (**1c**), [(dmba)Pd{Ph$_2$PCH···C(···O)Ph}] (**2a**), [(8-mq)Pd{Ph$_2$PCH···C(···O)Ph}] (**2b**), and [(8-mq)Pd{Ph$_2$PCH(AuPPh$_3$)(C(O)Ph}](BF$_4$) (**4b**) were prepared according to published procedures.[6,7,28−30]

Ph$_2$PCH$_2$C(O)(*p*-C$_6$H$_4$CH$_3$). A hexane solution (1.60 mol·L^{-1}) of ^{n}BuLi (60 mL, 0.096 mmol) was added dropwise at −70 °C to a solution of diisopropylamine (13.5 mL, 0.096 mmol) in THF (30 mL). After the mixture was stirred for 0.5 h, a solution of *p*-tolylacetophenone (12.7 mL, 0.095 mmol) in THF (20 mL) was added dropwise at −70 °C. After further stirring for 2.5 h, a solution of Ph$_2$PCl (17 mL, 0.095 mmol) in THF (30 mL) was added dropwise at −70 °C. The mixture was stirred overnight with a slow increase in temperature from −70 °C to room temperature. The solvent was removed *in vacuo*. The crude product was dissolved in toluene (100 mL). The colorless solution was filtered and concentrated, and addition of pentane afforded a white powder, which was filtered and dried *in vacuo*. White crystals were obtained from dry ethanol at −25 °C (13.0 g, 43%): mp 86 °C. IR (KBr): ν(CO) 1671 vs. ^{1}H NMR (CDCl$_3$): δ 7.9−7.2 (m, 14 H, aromatic), 3.79 (s, 2 H, PCH$_2$), 2.40 (s, 3 H, CH$_3$). ^{31}P{^{1}H} NMR (CDCl$_3$): δ −16.66 (s). Anal. Calcd for C$_{21}$H$_{19}$OP (M = 318.36): C, 79.23; H, 6.02. Found: C, 79.57; H, 6.11.

***cis*-[Ni{Ph$_2$PCH···C(···O)(*p*-C$_6$H$_4$CH$_3$}$_2$] (1b).** A mixture of NiCl$_2$·6H$_2$O (0.400 g, 1.68 mmol) and Ph$_2$PCH$_2$C(O)(*p*-C$_6$H$_4$CH$_3$) (1.070 g, 3.37 mmol) was stirred in EtOH (20 mL). A red suspension was formed, and after further stirring for 1 h, a solution of NaOEt (prepared from 0.135 g of Na and 10 mL of EtOH) was slowly added. After being stirred for 1 h, the orange suspension was cooled to 0 °C and filtered. The orange residue was washed with cold EtOH (10 mL), dried *in vacuo*, and used without further purification (1.117 g, 95%). IR (KBr): ν(C$^{\bullet\bullet}$C) + ν(C$^{\bullet\bullet}$O) 1524 s. ^{1}H NMR (CD$_2$Cl$_2$): δ 7.78−7.11 (m, 14 H, aromatic), 4.53 (s, 2 H, PCH), 2.37 (s, 6 H, CH$_3$). ^{31}P{^{1}H} NMR (CDCl$_3$): δ 28.4 (s). Anal. Calcd for C$_{42}$H$_{36}$NiO$_2$P$_2$ (M = 693.37): C, 72.76; H, 5.23. Found: C, 72.61; H, 5.07.

Formation of *cis*-[Pt{Ph$_2$PCH···C(···O)Ph}$_2$] (3) from 1a. A mixture of **1a** (0.100 g, 0.15 mmol) and [PtCl$_2$(COD)] (0.058 g, 0.015 mmol) was stirred in THF (10 mL) at 40 °C. After a few minutes, a white suspension was formed which was further stirred for 0.5 h at room temperature. The solvent was removed *in vacuo*. The white residue was extracted with CH$_2$Cl$_2$ (10 mL), filtered, and concentrated *in vacuo*. Addition of pentane afforded air-stable white needles. Product **3** (0.080 g, 66%) was characterized by comparison of its ^{1}H NMR and ^{31}P NMR data with those of an authentic sample.[7c]

[(dmba)Pd{Ph$_2$PCH(AuPPh$_3$)C(O)Ph}](BF$_4$) (4a). To a stirred solution of [AuCl(PPh$_3$)] (0.495 g, 1.00 mmol) in THF (100 mL) was added solid AgBF$_4$ (0.200 g, 1.00 mmol). After being stirred for 0.5 h, the reaction mixture was filtered. To the filtrate was added [(dmba)Pd{Ph$_2$PCH···C(···O)Ph}] (0.548 g, 1.00 mmol) and the solution was stirred for 2 h. The resulting solution was concentrated and addition of hexane afforded a white powder, which was washed with toluene and dried *in vacuo*. With the exclusion of light, a recrystallization from toluene/CH$_2$Cl$_2$/hexane afforded white crystals characterized as complex **4a**·0.5C$_7$H$_8$ (0.729 g, 77%). IR (KBr): ν(CO) 1581 w, 1506 s, ν(BF$_4$) 1101 s, 1084 vs, 1024 sh. IR (CD$_2$Cl$_2$): ν(CO) 1510 s. ^{1}H NMR (CD$_2$Cl$_2$): δ 8.23−6.73 (m, 34 H, aromatic), 5.23 (t, 1 H, PCH, ^2J(P$_{Pd}$H) = ^5J(P$_{Au}$H) = 8.2 Hz), 4.23 (dd, 1 H, CH^{A}N, part A of an ABX spin system (A = B = H, X = P), ^2J(AB) = 14.1 Hz, ^4J(AX) = 2.3 Hz), 4.01 (dd, 1 H, CH^{B}N, part B of an ABX spin system, ^2J(AB) = 14.1 Hz, ^4J(BX) < 2.04 Hz), 3.05 (d, 3 H, Me^{A}N, ^4J(PH) = 2.06 Hz), 2.98 (d, 3 H, Me^{B}N, ^4J(PH) = 2.04 Hz). ^{31}P{^{1}H} NMR (C$_6$D$_6$/CD$_2$Cl$_2$): δ 39.08 (s, 1 P), 39.06 (s, 1 P). Anal. Calcd for C$_{47}$H$_{44}$AuBF$_4$NOP$_2$Pd·0.5C$_7$H$_8$ (M = 1090.99 + 46.06): C, 53.34; H, 4.25; N, 1.23. Found: C, 53.21; H, 4.24; N, 1.26. FAB mass spectrum m/e 1002 (M − 2 H − BF$_4$), 544 (M − 2 H − BF$_4$ − AuPPh$_3$).

***cis*-[Ni{Ph$_2$PCH···C(···O)Ph}$_2$]CoI$_2$ (5a).** A mixture of complex **1a** (0.300 g, 0.45 mmol) and anhydrous CoI$_2$ (0.140 g, 0.45 mmol) was stirred for 3 h in Et$_2$O (20 mL). The green precipitate was filtered, washed with Et$_2$O (10 mL), and dried *in vacuo*. The crude product was dissolved in a 1:1 mixture of toluene/CH$_2$Cl$_2$ (1:1) (20 mL), and the solution was filtered and then concentrated *in vacuo*. On being cooled to −23 °C, the solution afforded dark green, air-stable crystals of **5a**·0.25C$_7$H$_8$ (0.365 g, 80%). IR (KBr): ν(C$^{\bullet\bullet}$C) + ν(C$^{\bullet\bullet}$O) 1551 vs, 1524 sh. ^{31}P{^{1}H} NMR (CD$_2$Cl$_2$, 298 K): δ −105.1 (s). Anal. Calcd for C$_{40}$H$_{32}$CoI$_2$NiO$_2$P$_2$·0.25C$_7$H$_8$ (M = 978.00 + 23.03): C, 50.09; H, 3.42. Found: C, 50.00; H, 3.27. FAB mass spectrum: *m/e* 978 (5%, M), 850 (60%, M − I), 793 (15%, M + 2H − Co − I), 665 (100%, M − CoI$_2$), 362 (40%, M$^+$ − 2I).

***cis*-[Ni{Ph$_2$PCH···C(···O)(*p*-C$_6$H$_4$CH$_3$}$_2$]CoI$_2$ (5b).** Following the procedure described for **5a**, but starting from **1b** (0.400 g, 0.43 mmol) and CoI$_2$ (0.135 g, 0.43 mmol), **5b**·0.25C$_7$H$_8$ was obtained as green crystals (0.580 g, 73%), which were suitable for X-ray analysis. IR (KBr): ν(C$^{\bullet\bullet}$C) + ν(C$^{\bullet\bullet}$O) 1548 s, 1505 s. ^{31}P{^{1}H} NMR (CD$_2$Cl$_2$, 298 K): δ −102.5 (s). Anal. Calcd for C$_{42}$H$_{36}$CoI$_2$NiO$_2$P$_2$·0.25C$_7$H$_8$

(28) Drew, D.; Doyle, J. R. *Inorg. Synth.* **1990**, *28*, 346−351.
(29) Braunstein, P.; Matt, D.; Nobel, D.; Balegroune, F.; Bouaoud, S. E.; Grandjean, D. Fischer, J. *J. Chem. Soc., Dalton Trans.* **1988**, 353−361.
(30) Georgiev, E. M.; tom Dieck, H.; Fendesak, G.; Hahn, G.; Petrov, G.; Kirilov, M. *J. Chem. Soc., Dalton Trans.* **1992**, 1311−1315.

Table 5. Crystallographic Data for Compounds **4a**·$^1/_2C_7H_8$ and **5b**·CH_2Cl_2

	4a·$^1/_2C_7H_8$	**5b**·CH_2Cl_2
mol formula	$[C_{47}H_{43}AuNOP_2Pd][BF_4]\cdot{}^1/_2C_7H_8$	$C_{40}H_{36}NiCoI_2P_2O_2\cdot CH_2Cl_2$
mol wt	1136.05	1066.3
cryst system	triclinic	monoclinic
space group	$P\bar{1}$	$P2_1/n$
radiattion	graphite-monochromated (Mo-Kα, $\lambda = 0.71073$ Å)	
a, Å	16.778(4)	12.940(1)
b, Å	14.269(5)	18.329(2)
c, Å	10.838(6)	18.495(2)
α, deg	79.27(4)	
β, deg	71.59(3)	91.627(8)
γ, deg	72.68(2)	
V, Å^3	2338(2)	4384.8(8)
Z	2	4
d_{calcd}, g cm^{-3}	1.614	1.617
$F(000)$	1122	2100
μ(Mo Kα), cm^{-1}	36.4	24.9
θ range, deg	3−26	2−23
no. of unique tot. data	9681	6079
no. of unique obsd data	7240 [$I > 2\sigma(I)$]	3644 [$I > 6\sigma(I)$]
R[a]	0.0363	0.040
R_w[b]	0.0406	0.038

[a] $R = \sum||F_o| - |F_c||/\sum|F_o|$. [b] $R_w = [\sum w(|F_o| - |F_c|)^2/\sum w(F_o)^2]^{1/2}$.

(M = 1006.11 + 23.03): C, 51.03; H, 3.72. Found: C, 50.80; H, 3.83.

***cis*-[Ni{$Ph_2PCH\cdots C(\cdots O)Me$}$_2$]$CoI_2$ (5c).** Following the procedure described for **5a**, but starting from **1c** (0.200 g, 0.37 mmol) and CoI_2 (0.116 g, 0.37 mmol), **5c**·0.25C_7H_8 was obtained as a green crystalline powder (0.140 g, 43%). IR (KBr): $\nu(C{=}C) + \nu(C{=}O)$ 1568 s. ^{1}H NMR (CD_2Cl_2, 298 K): δ 49.99 (s, 2 H, CHP), 15.34 (s, 8 $H_{m\ or\ o}$, Ph_2P), 10.45 (s, 8 $H_{o\ or\ m}$, Ph_2P), 9.75 (s, 4 H_p, Ph_2P), −83.86 (s, 6 H, CH_3). ^{31}P{^{1}H} NMR (CD_2Cl_2, 298 K): δ −78.4 (s). Anal. Calcd for $C_{30}H_{28}CoI_2NiO_2P_2\cdot 0.25C_7H_8$ (M = 853.89 + 23.03): C, 43.48; H, 3.45. Found: C, 43.17; H, 3.50.

***cis*- and *trans*-[Ni{$^iPr_2PCH\cdots C(\cdots O)Ph$}$_2$] (6).** Following the procedure described for **1b**, but starting from the ligand $^iPr_2PCH_2C(O)Ph$ (3.03 g, 12.82 mmol) and $NiCl_2\cdot 6H_2O$ (1.523 g, 6.41 mmol), **6** was obtained as orange-red crystals (2.05 g, 61%). IR (KBr): $\nu(C\cdots C) + \nu(C\cdots O)$ 1517 vs. Both isomers *cis*-**6** and *trans*-**6** were present in a ca. 1:1 ratio in $CDCl_3$. ^{1}H NMR ($CDCl_3$): δ 7.92−7.26 (m, 10 H, aromatic), 4.37 (s, 2 H, PCH, cis or trans isomer), 4.19 (s, 2 H, PCH, trans or cis isomer), 2.21 (m, 4 H, C*H*(CH_3)$_2$), 2.06 (m, 4 H, C*H*(CH_3)$_2$), 1.57−1.29 (m, 24 H, CH(C*H*$_3$)$_2$). ^{31}P{^{1}H} NMR ($CDCl_3$): δ 50.0 (s, 2 P, trans isomer) and 39.3 (s, 2 P, cis isomer). Anal. Calcd for $C_{28}H_{40}NiO_2P_2$ (M = 529.25): C, 63.55; H, 7.62. Found: C, 63.67; H, 7.64.

***cis*-[Ni{$^iPr_2PCH\cdots C(\cdots O)Ph$}$_2$]$CoI_2$ (7).** Following the procedure described for **5a**, but starting from **6** (0.200 g, 0.377 mmol) and anhydrous CoI_2 (0.118 g, 0.377 mmol), **7** was obtained as a green crystalline powder (0.240 g, 76%). IR (KBr): $\nu(C{=}C) + \nu(C{=}O)$ 1559 vs. ^{1}H NMR (CD_2Cl_2, 298 K): δ 52.05 (s, 2 H, CHP), 9.64 (s, 2 H, C*H*(CH_3)$_2$), 9.33 (s, 12 H, CH(C*H*$_3$)$_2$), 5.33 (s, 2 H, C*H*(CH_3)$_2$), 5.12 (s, 12 H, CH(C*H*$_3$)$_2$), −0.60 (s, 2 H_p, C_6H_4), −8.91 (s, 4 H_m, C_6H_4), −46.00 (s, 4 H_o, C_6H_4). ^{31}P{^{1}H} NMR (CD_2Cl_2, 298 K): δ −54.7 (s). Anal. Calcd for $C_{28}H_{40}CoI_2NiO_2P_2$ (M = 841.99): C, 39.94; H, 4.79. Found: C, 40.32; H, 4.66.

Crystal Structure Determinations for Compounds 4a·$^1/_2C_7H_8$ and 5b·CH_2Cl_2. The crystallographic data for both compounds are summarized in Table 5. Data were collected at room temperature (25 °C) on a Philips PW 1100 (**4a**·$^1/_2C_7H_8$) and on a Enraf Nonius CAD4 diffractometer (**5b**·CH_2Cl_2). One standard reflection was monitored every 100 measurements; no significant decay was noticed over the time of data collection. Intensities were corrected for the Lorentz−polarization effect and an empirical absorption correction was applied after isotropic convergence.[31,32] The structures were solved by direct and Fourier methods and refined by full-matrix least-squares methods, first with isotropic thermal parameters and then with anisotropic thermal parameters for all the non-hydrogen atoms excepting the carbon atoms of the toluene molecule of solvation of **4a**·$^1/_2C_7H_8$. The toluene molecule, lying on an inversion center, was found disordered with the methyl group distributed in two centrosymmetrically related positions. All hydrogen atoms (excepting those of the toluene molecule) were placed at their geometrically calculated positions and refined "riding" on the corresponding carbon atoms. The final cycles of refinement were carried out on the basis of 567 (**4a**·$^1/_2C_7H_8$) and 479 (**5b**·CH_2Cl_2) variables. The highest remaining peak in the final difference map was equivalent to about 1.1 (**4a**·$^1/_2C_7H_8$) and 0.8 (**5b**·CH_2Cl_2) e/Å^3. In the final cycles of refinement a weighting scheme $w = K[\sigma^2(F_o) + gF_o^2]^{-1}$ was used; at convergence the K and g values were 1.129 and 0.00095 (**4a**·$^1/_2C_7H_8$), and 0.038 and 0.00034 (**5b**·CH_2Cl_2) respectively. The analytical scattering factors, corrected for the real and imaginary parts of anomalous dispersion, were taken from ref 32. All calculations were carried out using the SHELX-76 and SHELXS-86 systems of crystallographic computer programs.[33] The final atomic coordinates for the non hydrogen atoms are given in Tables S-II (**4a**·$^1/_2C_7H_8$) and S-III (**5b**·CH_2Cl_2). The atomic coordinates of the hydrogen atoms are given in Tables S-II (**4a**·$^1/_2C_7H_8$) and S-III (**5b**·CH_2Cl_2), the thermal parameters are given in Tables S-IV (**4a**·$^1/_2C_7H_8$) and S-V (**5b**·CH_2Cl_2).

Acknowledgment. We thank the Centre National de la Recherche Scientifique (Paris) for financial support, the Ministère de l'Enseignement Supérieur et de la Recherche for a Ph.D. grant to J.A and F.I. and the Consiglio Nazionale delle Ricerche (Rome) for financial supports. Y.D. is grateful to J. Hubsch and L. Montesi for preliminary magnetic measurements performed at the Service Commun de Magnétisme de l'Université Henri Poincaré Nancy I, and M.D and P.R are also grateful to R. Poinssot (IPCMS) for magnetic measurements.

Supporting Information Available: Crystallographic data (Table S-I), atomic coordinates for the non hydrogen atoms (Tables S-II (**4a**·1/2C_7H_8) and S-III (**5b**·CH_2Cl_2)), atomic coordinates of the hydrogen atoms (Tables S-IV (**4a**·1/2C_7H_8) and S-V (**5b**·CH_2Cl_2)), thermal parameters (Tables S-VI (**4a**·1/2C_7H_8) and S-VII (**5b**·CH_2Cl_2)) and complete bond distances and angles (Tables S-VIII (**4a**·1/2C_7H_8) and S-IX (**5b**·CH_2Cl_2)) (19 pages). Ordering information is given on any current masthead page.

IC9513494

(31) Walker, N.; Stuart, D. *Acta Crystallogr., Sect. A* **1983**, *39*, 158.
(32) *International Tables for X-Ray Crystallography*; Kynoch Press: Birmingham, England, 1974; Vol. IV.
(33) *SDP Structure Determination Package*; Enraf Nonius: Delft, The Netherlands, 1977. Sheldrick, G. M. SHELX-76 Program for crystal structure determination, University of Cambridge, England, 1976; SHELXS-86 Program for the solution of crystal structures, University of Göttingen, 1986.